Inverted Organic Solar Cells Based On PTB7:PC70BM Bulk Heterojunction

Nidhi Sharma[1], Chandra Mohan Singh Negi[2], Varsha Yadav[1], Ajay Singh Verma[1], Veera Sadhu[1], and Saral K. Gupta[1a)]

[1]*Department of Physics, Banasthali Vidyapith, Banasthali 304022, INDIA*
[2]*Department of Electronics, Banasthali Vidyapith, Banasthali 304022, INDIA*
[a)]Corresponding author: gsaral@banasthali.in

Abstract. This paper reports the fabrication and characterization of bulk heterojunction inverted structured organic solar cell devices (OSC) with the architecture of ITO/ZnO/PTB7:$PC_{70}BM$/MoO3/Ag. The photovoltaic properties of OSC were examined through the analysis of various photovoltaic parameters, which includes the external quantum efficiency, short circuit current density (J_{sc}), and open circuit voltage (V_{oc}). The inverted structured OSC device showed the efficiency of 5.87 %. The achieved efficiency can be attributed to the better light harvesting capability, improved interfacial properties and improved charge collection efficiency. The AC impedance technique was employed to extract internal parameters of the fabricated devices. The obtained impedance curves evidently exhibit high-quality correlation between the obtained data and the curve fitting data.

INTRODUCTION

In comparison to the other sources of electric power, solar cells are drawing a lot of attention because they utilize resources of nature for producing electricity, which is green and clean energy with nearly zero emission. However, high manufacturing cost limits wide spread use of solar cells for power generation. Organic solar cells (OSCs) have emerged as the potential aspirants to reduce the production cost to fabricate efficient devices that generates green electricity as low temperature roll to roll solution processing printing techniques enable larger area production [1]. Nevertheless, the performance of OSC is still poorer compared to the conventional crystalline silicon-based energy conversion devices. The efficiency of OSC may be increased by various approaches, such as by improving the surface morphology, enhancing the light harvesting and minimizing the charge recombination occurring at the HTL/Active layer/ETL interfaces [2]. Poly (3-hexylthiophene-2,5-diyl) (P3HT) has widely been used as the standard donor and absorber material in OSCs for many years [3]. But P3HT hardly absorbs the sun light above 600 nm, limiting the efficiency of solar cell. The rapid enhancement in higher efficiencies has been primarily achieved through the development of low band gap (LBG) donor materials. Poly thieno-thiophenebenzodithio-phenes (PTBs) are some of the most widely examined materials for their applicability as donors for the fabrication of OSCs, because of their excellent optical, electrical, and thermal properties, and good chemical stability. Among those PTBs, higher efficiencies have been achieved by the use of poly [[4,8-bis(2-ethylhexyl)oxy] benzo [1,2-b:4,5-b'] dithiophene-2,6-diyl] [3-fluoro-2-[(2-ethylhexyl) carbonyl]thienophenediyl] (PTB7) as the absorber combined with[6,6] - phenyl C70 butyric acid methyl ester ($PC_{70}BM$) as an electron acceptor for conventional configuration devices [4,5]. Recently, inverted structured OSCs with electron accepting fullerene and the electron donating polymer as the active layer have drawn great interest because of the inherent device stability and enhanced performance [6-7]. In recent times, inverted OSCs have achieved high records of power conversion efficiencies (PCE) compared with the standard architecture OSCs [8-9]. The interface between active layer and both electrodes plays the crucial role of charge extraction and collection, which require appropriate energy level alignment. Therefore interfacial layers of materials with appropriate work function can be inserted between the electrodes and the active layer, which can improve the charge extraction and collection, thus enhance the PCE of the device. Some

metal oxides including V_2O_5, WO_3 and MoO_3 have been used as hole selective interfacial layer materials. These buffer layers leads to optimum inverted OPVs electrodes selectivity, resulting in higher Fill Factors (FF) more than 65 percent, and in a few cases in improved lifetime performance. In the current research, we evaluate the photovoltaic performance of the OSC with inverted architecture of ITO/ZnO/PTB7:PC_{70}BM/MoO_3/Ag. Here PTB7:PC_{70}BM blend forms bulk heterojunction, which is used as the photoactive layer. ZnO and MoO_3 layers are electron and hole selective interfacial layers, respectively.

EXPERIMENTAL DETAILS

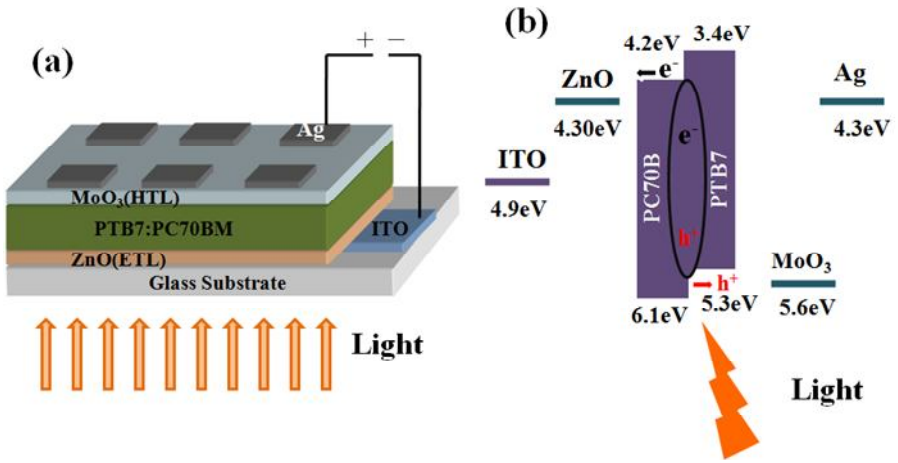

FIGURE 1. Schematic for an inverted organic solar cell structure and its corresponding energy level diagram.

Photovoltaic devices are fabricated using the following inverted architecture of ITO/ZnO/PTB7:PC71BM/MoO_3/Ag. Figure 1 shows the schematic for the OSC and the corresponding energy levels of the materials used to fabricate OSC. Firstly, ITO substrates are cleaned by ultrasonicator with detergent, DI water, and organic solvents, e.g. isopropanol and acetone (each for 10 min). The solution of ZnO was prepared with diethyl zinc and THF in 1:6 ratios. Then electron transport layer (ZnO) was spin-coated with 4000 rpm for 60s on patterned ITO substrate (sheet resistance of 15 Ω/square) and annealed at 110°C for 30 min. The photoactive layer was spin-coated from chlorobenzene (CB) solution at 1000 rpm for 1 min. The solutions of PTB7 and PC_{70}BM were mixed at 1:1.5 weight ratios with 20 mg/ml in DMF by stirring for 12 hrs. 1,8-Diiodooctane with a 3% volume ratio was added to the chlorobenzene solutions and stirred before use. A layer of MoO_3 (10nm) and silver (100nm) were deposited using thermal evaporator under a pressure of ~$6X10^{-7}$ mbar (using a shadow mask) forming the anode layer. The photoactive area of the cell was set to 10 mm^2. The solar cell characteristics were measured in a glove box, under nitrogen, using a Keithley 2602A source-meter with a 2-point probe technique. The photovoltaic cells were illuminated using a Simulator (LOT-Oriel), consisting a xenon lamp and a filter of AM 1.5G. External quantum efficiency has been measured using Enlitech with same set up inside the glove box.

RESULTS AND DISCUSSION

Fig. 2 (a) depicts the measured current-voltage (I-V) Properties of the fabricated OSC. The overall efficiency of power conversion (PCE) for the solar cell device is evaluated using several parameters, including short circuit current density (J_{sc}), fill factor (FF), and open circuit voltage (V_{oc}). The fabricated OSC exhibit a current density (J_{SC}) of 13.74mA cm^{-2}, V_{OC} of 0.75V, and FF of 56.9%, with a corresponding PCE of 5.87%. The photovoltaic performance of this inverted OSC surpasses the standard OSC using the same active layer material (J_{SC}=13.7 mA cm^{-2}, FF =40 %, V_{OC} =0.77 V, and PCE=4.42 %) reported elsewhere [11]. The better photovoltaic performance of inverted configuration is due to the more constructivecharge transport and improved charge collection efficiency compared with the normal structure [12-13]. The inverted architecture P3HT:PCBM BHJ based OSC using similar

interfacial layers and electrode configuration has shown PCE of 3.49%. The higher PCE compared than the P3HT:PCBM based OSC of similar architecture is indicative of better light harvesting capability of PTB7:$PC_{70}BM$ based OSC. As can be observed in Fig. 2 (b), the measured external quantum efficiency (EQE) of fabricated OSC has the wide spectral range from 300 nm to the 880 nm, while P3HT:PCBM based OSC demonstrates adequate EQE only in 400 to 650 nm wavelength range [14].

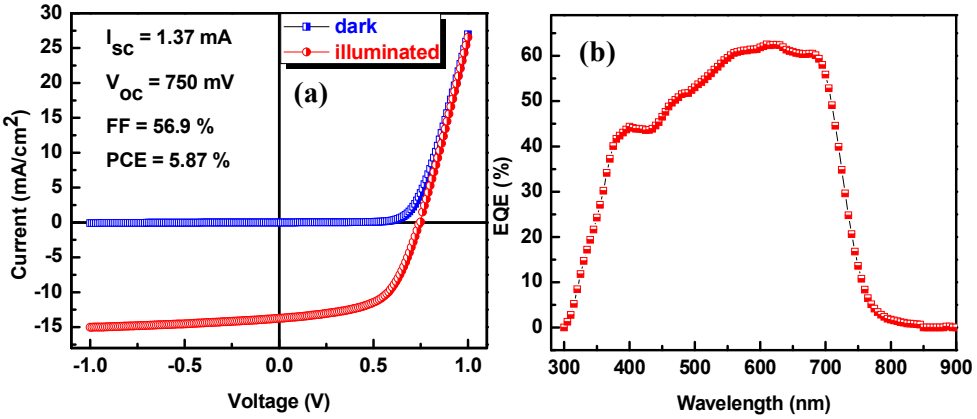

FIGURE 2(a). J-V curve under dark and illumination of ITO/ZnO/PTB7:$PC_{70}BM$/MoO3/Ag device, **(b)** External Quantum Efficiency curve of the device.

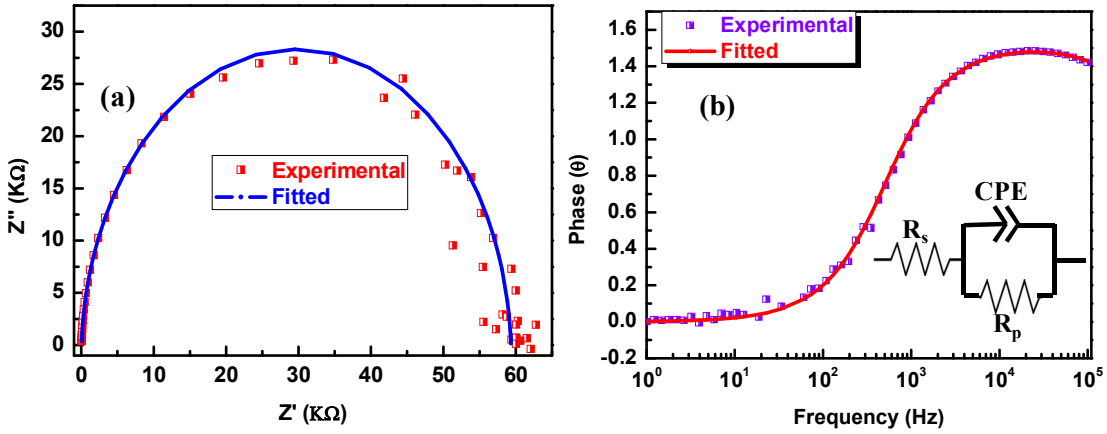

FIGURE 3. Impedance analysis of the solar cell device (a) Nyquist plots of PTB7:$PC_{70}BM$ based device (b) Bode plot of PTB7:$PC_{70}BM$ based device, inset figure of (b) shows electrical equivalent circuit that was used in simulation and curve fitting.

The measured impedance spectra under dark conditions at 0 V in terms of Cole-Cole plot and phase plot with corresponding fitted data obtained from the appropriate electrical equivalent circuit of solar cell [inset of Fig. 3 (b)] is displayed in Fig 3. The fitted curves exhibit good match with the measured experimental data. The parameters that extracted from the curves are listed in table 1. R_s in the circuit represent series resistance, R_p is the recombination resistance, and CPE model the imperfect capacitance which accounts the non-ideality resulting because of non-uniform non-homogeneous surface and interface, respectively, and distribution of current density. From the table 1, it can be observed that the device exhibits small R_s and large R_P signifying that better interface formation between the photoactive layer and electrodes. Better interface minimize charge trapping and recombination leading to the improved photovoltaic performance.

TABLE 1. The parameters extracted from the electrochemical impedance spectra of the OSC.

Device	$R_s(\Omega)$	$R_P(\Omega)$	CPE parameters		Capacitance (C_P)	τ_n (Sec.)
			Q_o	n	(μF)	
PTB7:PC70BM	32.29	59308	6.65 $X10^{-9}$	0.9704	.00377	2.23$X10^{-4}$

CONCLUSIONS

The inverted organic solar cell based on PTB7:$PC_{70}BM$ BHJ photoactive layer were fabricated and characterized, which shows PCE of 5.87%, J_{SC} of 13.74 $mAcm^{-2}$, V_{OC} of 0.75 V and FF of 56.9 %. The OSC showed high EQE in the range of 300 to 800 nm. The impedance analysis revealed that the device has comparatively smaller R_s and larger R_p, which is an indicative that the interfacial layer has improved the contact between electrodes and active layer. The light harvesting capability, better charge collection efficiency due to inverted architecture and improve interfacial properties, resulting into the PCE of 5.87 %.

ACKNOWLEDGEMENTS

The authors are grateful to the Department of Science and Technology (DST) for providing the financial support from under the CURIE program (grant No. SR/CURIE- Phase-III/01/2015(G)), and MHRD FAST program (grant No.5-5/2014-TS.VII), Govt. of India.

REFERENCES

1. J. Kusuma, and R. G. Balakrishna, Solar Energy **159**, 682-696(2018).
2. S. Lattante, Electronics **3**, 132-164 (2014).
3. W. Xu, C. Yi, X. Yao, L. Jiang, X. Gong, and Y. Cao, ACS Omega **2**, 1786-1794 (2017).
4. I. Etxebarria, J. Ajuria, and R. Pacios, Journal of Photonics for Energy **5**, 057214(2015).
5. K. Tada, Polymer Bulletin**73**, 2401-2408(2016).
6. G. J. Hedley, A. J. Ward,A.Alekseev, C. T. Howells, E. R. Martins,L. A. Serrano, G. Cooke, A. Ruseckas, and I. D. Samuel, Nature communications **4**, 2867(2013).
7. H. Zhou, Y. Zhang, J. Seifter, S. D. Collins, C. Luo, G. C. Bazan, T.Q. Nguyen, and A. J. Heeger, Advanced materials **25**,1646-1652 (2013).
8. A. J.Pearson, P. E. Hopkinson, E. Couderc, K .Domanski, M. Abdi-Jalebi, and N. C. Greenham, Organic Electronics **30**, 225-236(2016).
9. D. B. Staple, P. A. Oliver, and I. G. Hill, Physical Review B **89**, 205313(2014).
10. Y. Wang, H. Cong, B. Yu, Z. Zhang, and X. Zhan, Materials **10**, 1064(2017).
11. J. Farinhas, R. Oliveira, Q. Ferreira, J. Morgado, and A. Charas, International Journal of Photoenergy**2017**, (2017).
12. B. Ray, A. G. Baradwaj, M. R. Khan, B. W. Boudouris, and M. A. Alam, Proceedings of the National Academy of Sciences**112**, 11193-11198 (2015).
13. A.Yadav, A.Upadhyaya, S. K. Gupta, A. S.Verma, and C. M. S. Negi, Superlattices and Microstructures **120**, 788-795 (2018).
14. J. Ajuria, I. Etxebarria, W. Cambarau, U. Munecas, R. Tena-Zaera, J. C.Jimeno, and R. Pacios, Energy & Environmental Science **4**, 453-458 (2011).